Microbiology, Metabolites and Biotechnology
Journal home page:
MMB
The former ARMMT

6-Amino-4*H*-pyran derivatives as potential anti-microbial and amyloid aggregation inhibitory agents

Sara Nasiri[1], Amir Arasteh[1]*, Masoud Mokhtary[2]

[1] *Department of Biology, Ra. C., Islamic Azad University, Rasht, Iran.*
[2] *Department of Chemistry, Ra. C., Islamic Azad University, Rasht, Iran.*

Article Info

Document Type:
Research Paper

Received 19/04/2026
Received in revised form 02/06/2026
Accepted 13/06/2026

Published 17/06/2026

Keywords:
Alzheimer
6-amino-4H-pyran derivatives
Nano MgO
Anti–amyloid
Anti–microbial

Abstract

Pyran and its derivatives are an important group of heterocyclic compounds. These compounds are used in chemistry and pharmacy. This study investigates the anti-microbial and anti-Alzheimer's effects of 6-amino-4*H*-pyran derivatives. 6-amino-4*H*-pyran derivatives were produced from ethyl acetoacetate, with benzaldehydes and malononitrile in the presence of nano–MgO in water at 80 ºC by remarkable efficiency. MIC, MBC, and disc diffusion methods were performed to evaluate the antibacterial effects of five 6-amino-4H-pyran derivatives. The Congo red uptake method was used to determine the degree of inhibition of amyloid fibril production from Bovine serum albumin. For all five 6-amino-4*H*-pyran derivatives, the minimum inhibitory concentration for both *Escherichia coli* (PTCC 13301) and *Staphylococcus aureus* (PTCC 1112) was observed in a 1:8 (v/v) dilution rate (125 µg/ml), and the minimum bactericidal concentration in gram-negative and gram-positive bacteria was in a 1:4 (v/v) dilution rate (250 µg/ml). Also, the best inhibitory properties for amyloid fibrils were seen at 12%, 4%, 8%, 16%, and 12% (w/v) solutions for 4a–4e compounds, respectively. The most significant reduction in the production of amyloid fibrils was observed for benzyl 6-amino-4-(3-chlorophenyl)-5-cyano-2-methyl-4*H*-pyran- 3-carboxylate (4d). The identified antimicrobial activity and inhibition of amyloid fibril production by 6-amino-4*H*-pyran derivatives indicate a potential area for future therapeutic development. However, comprehensive studies are needed to establish their efficacy in addressing complications of infectious diseases and Alzheimer's.

1. Introduction

Pyran derivatives are groups of important heterocyclic compounds that are present in the structure of a large number of natural compounds and exhibit different biological activities. They are used in cosmetics and pigments, and also in biochemistry (D. Kumar *et al.*, 2017). Pyran derivatives have a wide range of biological activities such as anti–allergy, anti–cancer, anti–influenza virus, anti–coagulant, and also anti–bacterial (K. A. Kumar *et al.*, 2015; Mahdavi *et al.*, 2018). In addition, recent findings indicate that pyran derivatives could represent a promising scaffold for the development of therapeutic agents targeting neurological diseases such as Alzheimer's and Parkinson's disease (Pourshojaei *et al.*, 2019). 4*H*-pyran rings are unstable and no specimen has been found freely in nature so far; however, the 4*H*-pyran form can be found in maltol in pine leaves and kojic acid, which is made by yeast of the Aspergillus family (El-Kady, Zohri, & Hamed, 2014). The first compounds with such a structure were synthesized in 1896, in which the middle ring was *4H*-Pyran (Sharma *et al.*, 2015).

In amyloidosis, amyloid can be found in the kidneys, liver, brain, and other organs. It is believed that the pathogenesis of human neurodegenerative diseases, such as Alzheimer's and Parkinson's, is the result of the accumulation of insoluble amyloid plaques in nerve tissue (Ma *et al.*, 2022). Alzheimer's disease (AD) is a progressive and incurable neurodegenerative disease characterized by progressive and irreversible memory loss (Herling *et al.*, 2024). An imbalance between the production of amyloid *β*–peptide (Aβ) from the amyloid β precursor protein leads to the destruction of the endolysosomal system, autophagy, and the subsequent formation of autophagic vacuoles and damaged mitochondria in neurons. One of the most important proteins involved in AD is called amyloid precursor protein (APP), which is expressed in nervous system cells and is involved in cell binding, cell contact, and attachment to the extracellular matrix and skeleton. Studies have also shown that there is a strong interaction between β-amyloid and tau proteins. β–amyloid accumulations inside and outside neurons and intraneuronal hyperphosphorylated tau cause dendritic spines and synapse destruction, which ultimately leads to

*Corresponding author E-mail: arasteh@iau.ac.ir
DOI: 22104/mmb.2026.8200.1202
https://mmb.irost.ir/article_1708.html

memory loss in Alzheimer's patients (Khazaey *et al.*, 2017). Other pathological factors, such as glia–mediated inflammation and neuronal death in Alzheimer's disease, are known to lead to decreased neuronal function and consequent abnormalities (Ow & Dunstan, 2014).

Diseases associated with amyloid fibrils are broadly classified into degenerative diseases (such as Alzheimer's) and prion diseases (such as bovine dementia) (Winblad *et al.*, 2016). Amyloid plaques in the extracellular environment and neurofibrillary tangle (NFT) masses inside neurons are two major pathological features of AD in the brain, commonly associated with cerebral amyloid angiopathy (CAA) (Kövari, Herrmann, Hof, & Bouras, 2013). Treatment for amyloid disease is difficult and is currently limited to the management of symptoms, especially for inherited systemic amyloidosis. Most of the AD drug discovery has focused on the inhibition of Aβ production as a result of amyloidogenic APP treatment(Hampel *et al.*, 2021). The need to find new compounds with such properties led us to investigate the inhibitory properties for the production of amyloid fibrils, as well as the antibacterial properties of 6-amino-4*H*-Pyran derivatives. These derivatives include ethyl 6-amino-5-cyano-2-methyl-4-(phenyl)-4*H*-pyran-3-carboxylate (4a), ethyl 6-amino-5-cyano-2-methyl-4-(3-nitrophenyl)-4*H*-pyran-3-carboxylate (4b), ethyl 6-amino-5-cyano-2-methyl-4-(4-nitrophenyl)-4*H*-pyran-3-carboxylate (4c), benzyl 6-amino-4-(3-chlorophenyl)-5-cyano-2-methyl-4*H*-pyran- 3-carboxylate (4d), and ethyl 6-amino-4-(4-bromophenyl)-5-cyano-2-methyl 4*H*-pyran-3-carboxylates (4e).

The selection of the 6-amino-4H-pyran derivatives (4a–4e) in this study was guided by a systematic rationale based on the introduction of diverse substituents at the C-4 position of the pyran ring. Specifically, derivatives bearing electron-withdrawing groups (nitro, chloro, bromo) and an unsubstituted phenyl ring were chosen to evaluate the influence of electronic and steric effects on both antimicrobial and anti-amyloid activities. The choice of the 3-nitro (4b) and 4-nitro (4c) derivatives allowed a comparative assessment of positional isomerism, while the 3-chloro (4d) and 4-bromo (4e) analogs provided insight into the role of halogen substitution. This targeted structural variation was intended to establish a preliminary structure–activity relationship (SAR) and identify the most promising candidates for further development.

The present work introduces 6-amino-4H-pyran derivatives as a novel class of compounds with potential applications in mitigating complications of infectious diseases and Alzheimer's. Our literature search indicates that while the 6-amino-4H-pyran scaffold has not been extensively studied for anti-amyloid activity and related derivatives have shown limited success in this area, this study provides the first comprehensive report on the dual antimicrobial and anti-amyloid inhibitory potential of this specific derivative series (compounds 4a-4e). The pyran scaffold, known for its versatile biological profile, offers a promising platform for the development of multifunctional agents.

Accordingly, we hypothesized that certain structural features within this class of compounds could confer dual activity, potentially leading to candidates with broader therapeutic applicability. This rationale provides a unified framework for investigating both endpoints within a single study and strengthens the significance of our findings.

2. Materials and Methods

2.1. Materials

All chemicals and reagents were of analytical grade unless otherwise specified. Specific reagents were sourced as follows: Benzaldehyde, Purity: ≥ 99%, Grade: Analytical Reagent (AR), Merck (Darmstadt, Germany). Ethyl acetoacetate, Purity: ≥ 99%, Grade, Sigma-Aldrich, and Benzyl acetoacetate, Purity: HPLC Grade, Merck (Darmstadt, Germany).

Fourier transform infrared (FTIR) spectra were recorded with a Shimadzu FTIR spectrometer (8900, Japan) using KBr pellets. NMR spectra were recorded in $CDCl_3$ solution using a Bruker Advance DRX 400 MHz spectrometer.

2.2. Synthesis of 6-amino-5-cyano-4H-pyran derivatives

6-Amino-5-cyano-4H-pyran derivatives were synthesized as follows: A mixture of ethyl acetoacetate or benzyl acetoacetate (1 mmol), benzaldehyde (1 mmol), and malononitrile (1 mmol) in the presence of nano-MgO (0.01 g) was stirred at 500 rpm in water (100 mL) at 80 °C for 30 min. Upon completion, the mixture was cooled, and the crude product was purified by recrystallization from ethanol to afford the corresponding 6-amino-4-aryl-5-cyano-2-methyl-4H-pyran-3-carboxylates. The products 4a–4e were obtained in 85, 90, 88, 82, 91% yields, respectively.

The nano-MgO catalyst was characterized by X-ray diffraction (XRD) and transmission electron microscopy (TEM). This method offers an improved approach for the synthesis of 6-amino-4H-pyran derivatives without the use of toxic catalysts or solvents (Sojoudi & Mokhtary, 2018).

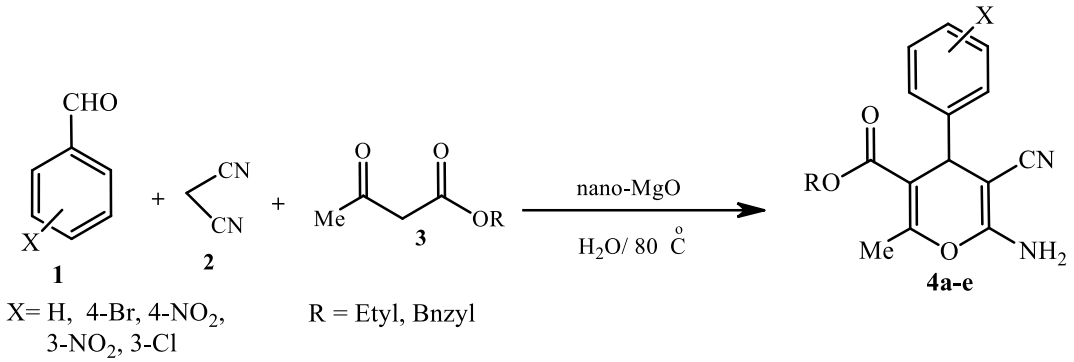

Scheme 1. Synthesis of 6-amino-5-cyano-4H-pyran derivatives

2.3. Spectral data of compounds

All synthesized compounds were characterized by FT-IR and NMR spectroscopy.

ethyl 6-amino-5-cyano-2-methyl-4-(phenyl)-4H-pyran-3-carboxylate (4a):

Yellow solid; mp 193–195 °C. FT-IR (KBr, cm^{-1}): 3407, 3328 (N–H stretch), 2192 (C≡N stretch), 1687 (C=O stretch), 1608, 1481 (C=C aromatic stretch), 1261 (C–N stretch), 1066 (C–O stretch), 837 (C–H out-of-plane bending, aromatic). ^{1}H NMR ($CDCl_3$, 400 MHz): δ 7.43–7.25 (m, 5H, Ar–H), 4.54 (br s, 2H, NH_2), 4.43 (s, 1H, H4), 4.07 (q, 2H, J = 7.1 Hz, OCH_2CH_3), 2.39 (s, 3H, CH_3), 1.11 (t, 3H, J = 7.1 Hz, OCH_2CH_3). ^{13}C NMR ($CDCl_3$, 100 MHz): δ 165.2, 157.6, 155.8, 143.9, 128.5 (2C), 127.8 (2C), 126.9, 117.8, 105.3, 60.3, 58.7, 37.2, 17.8.

ethyl 6-amino-5-cyano-2-methyl-4-(3-nitrophenyl)-4H-pyran-3-carboxylate (4b):

Yellow solid; mp 184–186 °C. FT-IR (KBr, cm^{-1}): 3400, 3300 (N–H stretch), 2190 (C≡N stretch), 1690 (C=O stretch), 1610, 1470 (C=C aromatic stretch), 1550, 1350 (NO_2 asymmetric stretch), 1250 (C–N stretch), 1050 (C–O stretch), 790, 690 (C–H out-of-plane bending, aromatic). ^{1}H NMR ($CDCl_3$, 400 MHz): δ 8.11 (d, 1H, J = 8.1 Hz, H2″), 8.05 (t, 1H, J = 2.0 Hz, H4″), 7.59 (d, 1H, J = 7.6 Hz, H6″), 7.50 (t, 1H, J = 7.9 Hz, H5″), 4.63 (br s, 2H, NH_2), 4.58 (s, 1H, H4), 4.06 (q, 2H, J = 7.1 Hz, OCH_2CH_3), 2.41 (s, 3H, CH_3), 1.12 (t, 3H, J = 7.1 Hz, OCH_2CH_3). ^{13}C NMR ($CDCl_3$, 100 MHz): δ 164.8, 158.0, 156.2, 148.3, 145.8, 134.2, 129.3, 122.8, 122.0, 117.3, 105.6, 60.8, 58.9, 37.0, 17.6.

ethyl 6-amino-5-cyano-2-methyl-4-(4-nitrophenyl)-4H-pyran-3-carboxylate (4c):

Orange solid; mp 178–180 °C. FT-IR (KBr, cm^{-1}): 3400, 3330 (N–H stretch), 2196 (C≡N stretch), 1687 (C=O stretch), 1602, 1450 (C=C aromatic stretch), 1517, 1340 (NO_2 asymmetric stretch), 1261 (C–N stretch), 1058 (C–O stretch), 820 (C–H out-of-plane bending, aromatic). ^{1}H NMR ($CDCl_3$, 400 MHz): δ 8.18 (d, 2H, J = 8.5 Hz, H3″, H5″), 7.38 (d, 2H, J = 8.5 Hz, H2″, H6″), 4.59 (br s, 2H, NH_2), 4.57 (s, 1H, H4), 4.04 (q, 2H, J = 7.1 Hz, OCH_2CH_3), 2.42 (s, 3H, CH_3), 1.10 (t, 3H, J = 7.1 Hz, OCH_2CH_3). ^{13}C NMR ($CDCl_3$, 100 MHz): δ 164.7, 158.2, 156.3, 150.2, 147.1, 129.1 (2C), 124.0 (2C), 117.2, 105.7, 60.9, 59.1, 37.1, 17.5.

benzyl 6-amino-4-(3-chlorophenyl)-5-cyano-2-methyl-4H-pyran- 3-carboxylate (4d)

Yellow solid; mp 168–170 °C. FT-IR (KBr, cm^{-1}): 3396, 3326 (N–H stretch), 2190 (C≡N stretch), 1681 (C=O stretch), 1604, 1460 (C=C aromatic stretch), 1265 (C–N stretch), 1060 (C–O stretch), 790, 698 (C–H out-of-plane bending, aromatic). ^{1}H NMR ($CDCl_3$, 400 MHz): δ 7.41 (s, 1H, H2″), 7.30 (s, 5H, benzyl Ar–H), 7.24–7.19 (m, 2H, H4″, H6″), 7.15–7.10 (m, 1H, H5″), 5.05 (d, 1H, J = 12.2 Hz, OCH_2Ph), 4.98 (d, 1H, J = 12.2 Hz, OCH_2Ph), 4.51 (br s, 2H, NH_2), 4.41 (s, 1H, H4), 2.40 (s, 3H, CH_3). ^{13}C NMR ($CDCl_3$, 100 MHz): δ 164.3, 156.9, 156.4, 144.7, 134.1, 133.4, 128.8, 128.5 (2C), 128.3 (2C), 128.2, 127.4, 126.5, 124.8, 117.5, 105.9, 65.7, 60.6, 37.4, 17.5.

ethyl 6-amino-4-(4-bromophenyl)-5-cyano-2-methyl 4H-pyran-3-carboxylates (4e):

Yellow solid; mp 170–172 °C. FT-IR (KBr, cm^{-1}): 3407, 3328 (N–H stretch), 2192 (C≡N stretch), 1687 (C=O stretch), 1608, 1481 (C=C aromatic stretch), 1261 (C–N stretch), 1066 (C–O stretch), 837 (C–H out-of-plane bending, aromatic). ^{1}H NMR ($CDCl_3$, 400 MHz): δ 7.45 (d, 2H, J = 8.4 Hz, H2″, H6″), 7.15 (d, 2H, J = 8.4 Hz, H3″, H5″), 4.56 (br s, 2H, NH_2), 4.39 (s, 1H, H4), 4.06 (q, 2H, J = 7.1 Hz, OCH_2CH_3), 2.37 (s, 3H, CH_3), 1.11 (t, 3H, J = 7.1 Hz, OCH_2CH_3). ^{13}C NMR ($CDCl_3$, 100 MHz): δ 165.0, 157.8, 156.0, 143.1, 131.7 (2C), 129.8 (2C), 121.2, 117.6, 105.5, 60.5, 58.8, 37.0, 17.7.

2.4. Investigation of antimicrobial activity

The antibacterial activity of the synthesized compounds was evaluated against *Escherichia coli* (PTCC 13301) and *Staphylococcus aureus* (PTCC 1112), obtained from the Iranian Institute of Standards and Industrial Research. Bacterial inocula were prepared in sterile saline and adjusted to 0.5 McFarland turbidity standard (1.5×10^8 CFU/mL). Minimum inhibitory concentration (MIC) was determined by the broth microdilution method according to CLSI guidelines (M07-A9). A stock solution of each compound (1 mg/mL) was prepared in dimethylformamide (DMF) and serially diluted two-fold in Mueller-Hinton broth to achieve final concentrations

ranging from 500 to 1.95 µg/mL. Tubes containing 2 mL of MHB, 200 µL of bacterial suspension, and the appropriate compound dilution were incubated at 37 °C for 24 h. The MIC was recorded as the lowest concentration with no visible turbidity. For MBC determination, aliquots from tubes with no visible growth were cultured on nutrient agar and incubated at 37 °C for 24–48 h; the MBC was defined as the lowest concentration with no colony growth. In the disk diffusion assay (CLSI M02-A12), sterile blank disks (6 mm) were impregnated with 50 µL of each compound solution (1 mg/mL in DMF) and placed on Mueller-Hinton agar plates inoculated with bacterial suspensions. DMF alone served as the solvent control, and gentamicin and tetracycline disks were used as positive controls. Plates were incubated at 37 °C for 24 h, and inhibition zone diameters were measured in millimeters. All experiments were performed in triplicate, and results are expressed as mean ± standard deviation (SD). Statistical analysis was carried out using one-way ANOVA, with $p < 0.05$ considered statistically significant (Balouiri *et al.*, 2016).

2.5. Investigation of anti–amyloid activity

Congo red spectrophotometry was used to detect amyloid fibril formation (Arasteh *et al.*, 2012). A stock solution of bovine serum albumin (BSA, 20 mg/mL) was prepared in citrate–phosphate buffer (pH 3.0). An aliquot of 100 µL of this stock solution was added to 300 µL of citrate–phosphate buffer (pH 3.0) containing 0, 20, 40, 60, 80, or 100 µL of each synthetic compound (4a–4e) solution (1 mg/mL in DMF). The total volume was adjusted to 500 µL with citrate–phosphate buffer, yielding final compound concentrations of 0, 40, 80, 120, 160, and 200 µg/mL, respectively, with a final BSA concentration of 4 mg/mL. Microtubes were agitated at 100 rpm for 48 h at 70 °C. After incubation, 100 µL of each sample was added to 1900 µL of Congo red buffer (20 µM Congo red in 5 mM phosphate buffer, 150 mM NaCl, pH 7.4) and incubated for 30 min at room temperature. Absorbance spectra were recorded from 400 to 600 nm. The absorbance at 540 nm, corresponding to the maximum absorbance of the Congo red–amyloid complex, was used as a measure of fibril formation. All experiments were performed in triplicate, and results are expressed as mean ± standard deviation (SD). Statistical analysis was performed using one-way ANOVA followed by Tukey's post hoc test, with $p < 0.05$ considered statistically significant. The selected conditions (pH 3, 70 °C, 48 h) are established in the literature for inducing BSA amyloid fibril formation under acidic denaturing conditions (Arasteh *et al.*, 2012; Bhattacharya *et al.*, 2011; Juárez *et al.*, 2009).

3. Results and Discussion

3.1. Antimicrobial effects

The antimicrobial activity of compounds 4a–4e was evaluated against *Escherichia coli* (Gram-negative) and *Staphylococcus aureus* (Gram-positive) using MIC, MBC, and disk diffusion assays (Table 1). The minimum inhibitory concentration (MIC) for all five compounds was 125 µg/mL against both bacterial strains, corresponding to a 1/8 dilution of the stock solution. The minimum bactericidal concentration (MBC) was 250 µg/mL (1/4 dilution) for both strains. No bacterial growth was observed in the negative control (medium without bacterial inoculum), and the solvent control (DMF alone) showed no inhibition, confirming that the observed activity was solely due to the synthetic compounds.

The antibacterial activity of 6-amino-4H-pyran derivatives has been previously attributed to the presence of the cyano and ester functional groups, which can interfere with bacterial cell wall synthesis and enzyme activity (Kumar *et al.*, 2017; Bhat *et al.*, 2018). Compared to standard antibiotics, the synthesized compounds exhibited moderate activity. For instance, while gentamicin and tetracycline typically show MIC values in the range of 0.5–8 µg/mL against *E. coli* and *S. aureus* (CLSI, 2020), the MIC of 125 µg/mL observed for compounds 4a–4e is higher. However, these values are comparable to those reported for similar 4H-pyran derivatives. Saeed *et al.* (2019) reported MIC values of 62.5–250 µg/mL for a series of 6-amino-4H-pyran-3-carboxylates against *S. aureus* and *E. coli*, which align well with our findings. Furthermore, the presence of electron-withdrawing groups such as nitro and chloro substituents on the aryl ring has been shown to enhance antibacterial activity (Rao *et al.*, 2020).

Figure 1. Growth inhibition halo in *E. coli* and *S. aureus* bacteria in the presence of synthetic product 4a

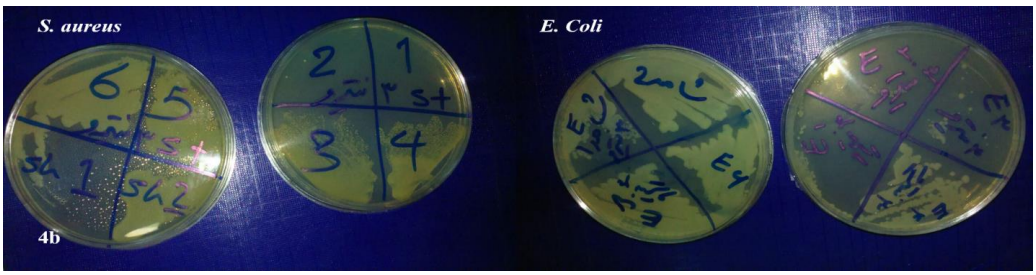

Figure 2. Growth inhibition halo in *E. coli* and *S. aureus* bacteria in the presence of synthetic product 4b

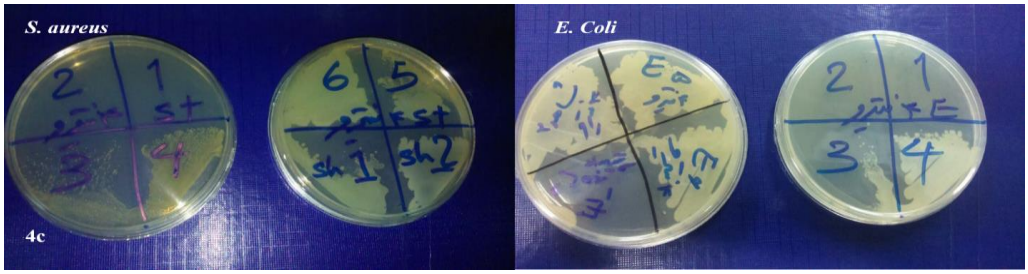

Figure 3. Growth inhibition halo in *E. coli* and *S. aureus* bacteria in the presence of synthetic product 4c

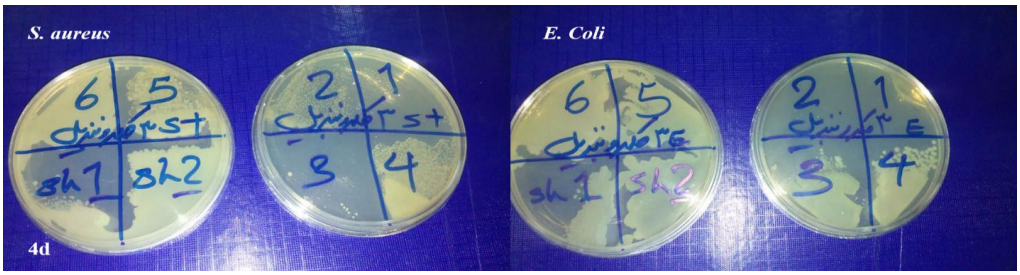

Figure 4. Growth inhibition halo in *E. coli* and *S. aureus* bacteria in the presence of synthetic product 4d

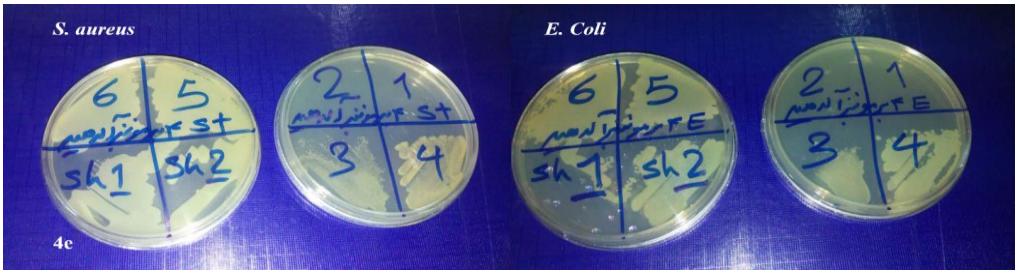

Figure 5. Growth inhibition halo in *E. coli* and *S. aureus* bacteria in the presence of synthetic product 4e

Table 1. *Growth Inhibition Halo, MIC, and MBC for* 6-amino-4H-pyran Derivatives

Compounds	**Antimicrobial test**	***E. Coli***	***S. aureus***
4a	Growth inhibition halo (mm)	5	2
	MIC (µg/ml)	125	125
	MBC (µg/ml)	250	250
4b	Growth inhibition halo (mm)	2	1
	MIC (µg/ml)	125	125
	MBC (µg/ml)	250	250
4c	Growth inhibition halo (mm)	2	4
	MIC (µg/ml)	125	125
	MBC (µg/ml)	250	250
4d	Growth inhibition halo (mm)	3	6
	MIC (µg/ml)	125	125
	MBC (µg/ml)	250	250
4e	Growth inhibition halo (mm)	4	1
	MIC (µg/ml)	125	125
	MBC (µg/ml)	250	250
Tetracycline	Growth inhibition halo (mm)	36	38
	MIC (µg/ml)	15	15

	MBC (µg/ml)	31	31
Gentamicin	Growth inhibition halo (mm)	24	24
	MIC (µg/ml)	15	15
	MBC (µg/ml)	31	31

In our study, compounds 4b (3-NO_2), 4c (4-NO_2), and 4d (3-Cl) did not show significantly lower MIC values compared to 4a (H) and 4e (4-Br), suggesting that within this series, the substitution pattern had a limited effect on antibacterial potency under the tested conditions.

3.2. Anti–amyloid effects

The anti-amyloid activity of compounds 4a–4e was evaluated by measuring the absorbance of the Congo red–amyloid complex at 540 nm after incubation of BSA with each compound at various concentrations (Figures 6–10, Table 2). Increasing concentrations of each compound led to a progressive reduction in absorbance intensity at 540 nm, indicating inhibition of amyloid fibril formation. The final concentrations of the compounds tested were 40, 80, 120, 160, and 200 µg/mL, corresponding to 4%, 8%, 12%, 16%, and 20% (v/v) of the stock solution (1 mg/mL) in the reaction mixture, respectively. Among all compounds, 4d (benzyl 6-amino-4-(3-chlorophenyl)-5-cyano-2-methyl-4H-pyran-3-carboxylate) exhibited the greatest inhibition, reducing the absorbance intensity by 62% at 200 µg/mL compared to the control. Compound 4b showed the highest inhibitory effect at 40 µg/mL (56% reduction), while 4c showed optimal inhibition at 80 µg/mL (48% reduction). Compounds 4a and 4e exhibited moderate inhibition, with maximal effects at 120 µg/mL (41% and 44% reduction, respectively). Statistical analysis (one-way ANOVA with Tukey's post hoc test) revealed that the differences between compounds were statistically significant at their optimal concentrations (Table 2). Specifically, 4d showed significantly greater inhibition compared to 4a (p = 0.008), 4c (p = 0.015), and 4e (p = 0.032), while the difference between 4d and 4b was not statistically significant (p = 0.064). These results suggest that the benzyl ester moiety and the 3-chloro substituent in 4d contribute to enhanced anti-amyloid activity.

AD is now considered a global health problem; therefore, the National Institute on Aging-Alzheimer's Association reclassified and updated the NINCDS–ADRDA criteria in 1984 to have greater specificity, sensitivity, and early identification of patients at risk of developing AD (Breijyeh & Karaman, 2020). Due to the amyloid plaques inside neurons, which result in AD in the brain, the anti-amyloid compound will be helpful in this process. On the other hand, anti–amyloid trials have failed in recent years, and the amyloid hypothesis has been challenged, with the number of phase 3 anti-amyloid trials decreasing significantly in 2019. Targets of phases 1 and 2 are diverse, and there is an increasing trend toward neuroprotective and anti–inflammatory targets. In phase 1 and phase 2 trials, respectively. Chronic progressive disorders often require two or more drugs to effectively slow disease progression. Potentially, it may be reasonable to conduct trials with a drug with multiple targets, namely anti–drug effects, neurotransmitter modulation, anti–inflammatory and protective effects (Huang *et al.*, 2020).

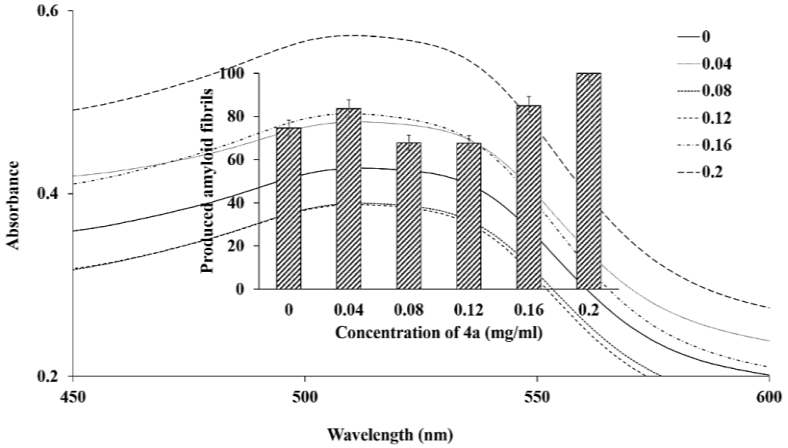

Figure 6. Congo red absorption spectrum and produced amyloid fibrils at different concentrations of 4a.

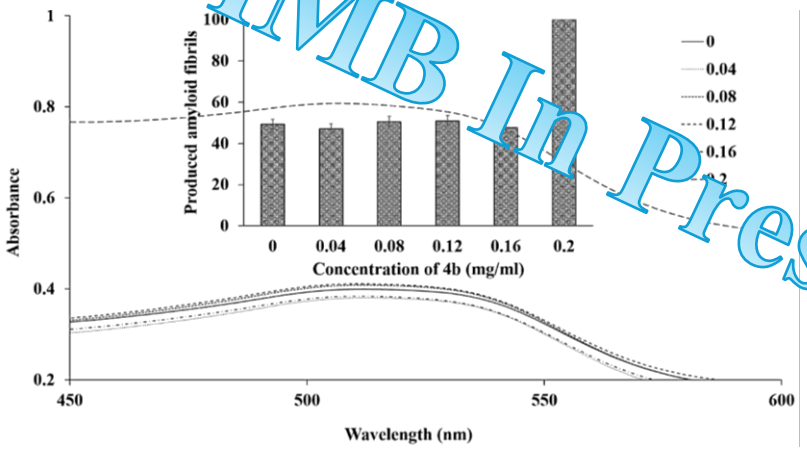

Figure 7. Congo Red Absorption Spectrum and Produced Amyloid Fibrils at Different Concentrations of 4b.

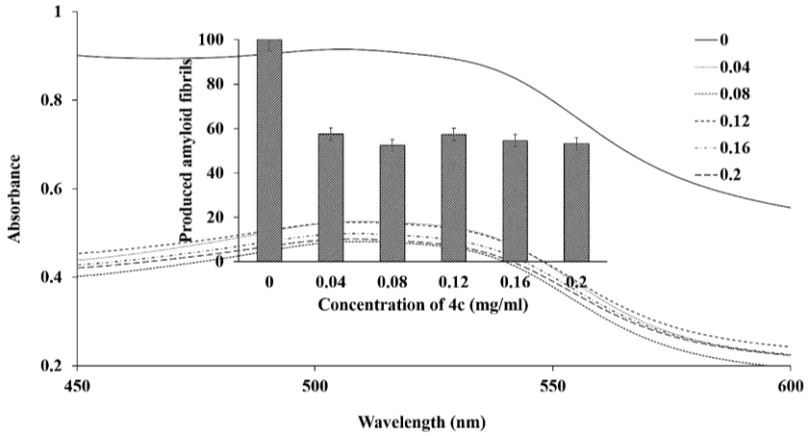

Figure 8. Congo red absorption spectrum and produced amyloid fibrils at different concentrations of 4c.

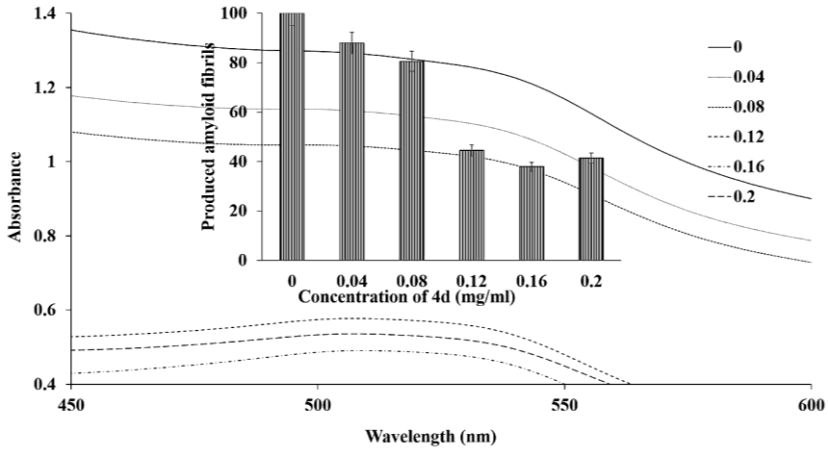

Figure 9. Congo red absorption spectrum and produced amyloid fibrils at different concentrations of 4d.

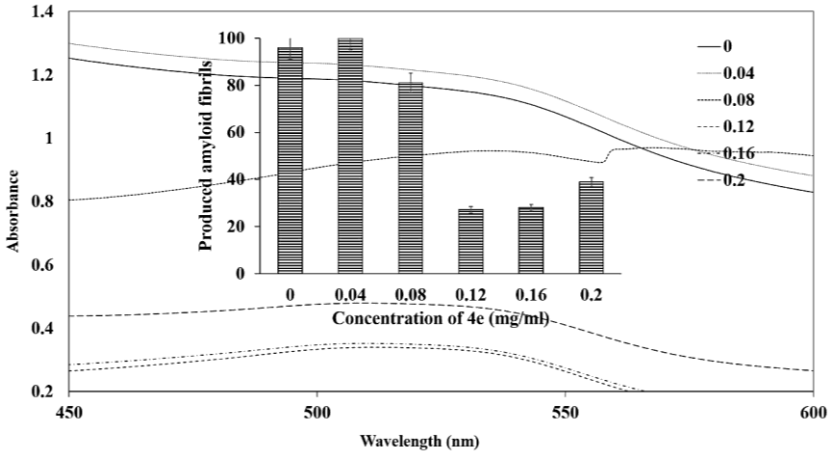

Figure 10. Congo red absorption spectrum and produced amyloid fibrils at different concentrations of 4e.

Table 2. Amounts of Produced Amyloid Fibrils (%) for Compounds 4a–4e at Various Concentrations.

Number	Produced Amyloid Fibrils for 4a (%)*	Produced Amyloid Fibrils for 4b (%)*	Produced Amyloid Fibrils for 4c (%)*	Produced Amyloid Fibrils for 4d (%)*	Produced Amyloid Fibrils for 4e (%)*
1	47.67±2.35	49.30±2.335	100±2.338	100±2.135	95.89±2.352
2	83.53±4.384	47.05±2.395	57.48±2.584	87.97±3.852	100±4.855
3	67.9±3.856	50.55±2.544	52.45±1.946	80.60±3.683	81.04±2.964
4	67.67±3.584	50.97±2.622	57.26±2.625	44.54±2.64	27.09±1.652
5	85.05±4.058	47.57±1.052	54.53±2.09	37.84±2.522	28.01±1.522
6	100±0.548	100±1.846	53.11±2.546	41.38±2.649	38.88±1.123

*Values are presented as mean ± standard error of the mean (SEM) from three independent experiments (n = 3).

A case–control (control group with amyloid injection, and case group with amyloid injection and proline–rich peptide 1 (PRP-1)) study reported a protective effect of hypothalamic PRP-1 on β-amyloid–induced AD in rats (Khalaji *et al.*, 2017). According to studies, some compounds that have a limiting effect on amyloid filament production can perform a protective role for AD (Freyssin *et al.*, 2017).

There is no comprehensive study on the issue of pyran derivative impact on amyloid fibril production and their anti-Alzheimer effects. In this regard, putting aside the antibacterial activity of 6-amino-4*H*-pyran derivatives, we demonstrated some anti–amyloid function at various concentrations, which is a glimpse into the future as a possible treatment for amyloid–induced AD. Meanwhile, almost all of the drug candidates tested for AD to date have not shown any efficacy, and there is a lack of *in vivo* and *in vitro* information, so further investigations on the anti–amyloid properties of 6-amino-4*H*-pyran derivatives are demanded. Studies on the impact of pyran derivatives on amyloid fibril production and their potential anti-Alzheimer effects remain limited. In this study, in addition to evaluating the antibacterial activity of 6-amino-4H-pyran derivatives, we investigated their anti-amyloid function at various concentrations. These findings offer a preliminary perspective on the potential application of these compounds as therapeutic candidates for amyloid-induced Alzheimer's disease.

4. Conclusion

In this study, a series of 6-amino-4H-pyran derivatives (4a–4e) was synthesized and evaluated for their antibacterial and anti-amyloid activities. Among the compounds tested, benzyl 6-amino-4-(3-chlorophenyl)-5-cyano-2-methyl-4H-pyran-3-carboxylate (4d) exhibited the most pronounced reduction in amyloid fibril production, suggesting that the benzyl ester and 3-chlorophenyl substituents may contribute favorably to anti-amyloid activity.

Additionally, all derivatives demonstrated moderate to good antibacterial activity against both Gram-positive (S. aureus) and Gram-negative (E. coli) strains. These findings indicate that 6-amino-4H-pyran derivatives represent a promising scaffold worthy of further investigation for applications in infectious disease and neurodegenerative disorder research. However, further studies, including in vivo evaluations, cytotoxicity assays, and mechanistic investigations, are necessary to fully assess their therapeutic potential. Future work should also explore structural modifications to optimize the bioactivity of this class of compounds.

Conflict of interest

The authors declare no conflict of interest.

Acknowledgment

Technical support by Rasht Branch, Islamic Azad University is gratefully acknowledged.

Ethical approval

This article does not contain any studies with human participants or animals performed by any of the authors.

Open access

Funding

None declared.

Authors' Contributions

SN: Investigation, Visualization, Roles/Writing – original draft; AA: Formal analysis; Investigation, Writing & editing, Roles; MM: Visualization, Methodology. All authors have read and approved the final version of the manuscript.

References

Arasteh, A., Habibi-Rezaei, M., Ebrahim-Habibi, A., & Moosavi-Movahedi, A. A. (2012). Response surface methodology for optimizing the bovine serum albumin fibrillation. *The Protein Journal, 31*(6), 457–465. https://doi.org/10.1007/s10930-012-9422-9

Balouiri, M., Sadiki, M., & Ibnsouda, S. K. (2016). Methods for in vitro evaluating antimicrobial activity: A review. *Journal of Pharmaceutical Analysis, 6*(2), 71–79. https://doi.org/10.1016/j.jpha.2015.11.005

Breijyeh, Z., & Karaman, R. (2020). Comprehensive review on Alzheimer's disease: Causes and treatment. *Molecules, 25*(24), Article 5789. https://doi.org/10.3390/molecules25245789

El-Kady, I. A., Zohri, A. N. A., & Hamed, S. R. (2014). Kojic acid production from agro-industrial by-products using fungi. *Biotechnology Research International, 2014*. https://doi.org/10.1155/2014/642385

Freyssin, A., Page, G., Fauconneau, B., & Bilan, A. R. (2018). Natural polyphenols effects on protein aggregates in Alzheimer's and Parkinson's prion-like diseases. *Neural Regeneration Research, 13*(6), 955. https://doi.org/10.4103/1673-5374.233432

Hampel, H., Vassar, R., De Strooper, B., Hardy, J., Willem, M., Singh, N., *et al.* (2021). The β-secretase BACE1 in Alzheimer's disease. *Biological Psychiatry, 89*(8), 745–756.

Huang, L.-K., Chao, S.-P., & Hu, C.-J. (2020). Clinical trials of new drugs for Alzheimer disease. *Journal of Biomedical Science, 27*(1), 1–13. https://doi.org/10.1186/s12929-023-00976-6

Khalaji, N., Sarkissian, J., Chavushyan, V., & Sarkisian, V. (2017). Protective effects of proline–rich peptide in a rat model of Alzheimer disease: An electrophysiological study. *Basic and Clinical Neuroscience, 8*(1), 5. https://doi.org/10.1155/2017/3948685

Khazaey, M. R., Habibi-Rezaei, M., Safarian, S., Karami, Z., & Sabouni, F. (2010). AGE proteins as a causative factor in Alzheimer's disease. *Iranian Journal of Pharmaceutical Research, Supplement*(1), 79–79.

Khonacha, S. E., Janahmadi, M., & Motamedi, F. (2019). Kisspeptin-13 improves spatial memory consolidation and retrieval against amyloid-β pathology. *Iranian Journal of Pharmaceutical Research: IJPR, 18*(Suppl 1), 169. https://doi.org/10.1016/j.neuroscience.2019.07.014

Kövari, E., Herrmann, F. R., Hof, P. R., & Bouras, C. (2013). The relationship between cerebral amyloid angiopathy and cortical microinfarcts in brain ageing and Alzheimer's disease. *Neuropathology and Applied Neurobiology, 39*(5), 498–509. https://doi.org/10.1111/nan.12003

Kumar, D., Sharma, P., Singh, H., Nepali, K., Gupta, G. K., Jain, S. K., *et al.* (2017). The value of pyrans as anticancer scaffolds in medicinal chemistry. *RSC Advances, 7*(59), 36977–36999. https://doi.org/10.1039/C7RA07845A

Kumar, K. A., Renuka, N., Kumar, G. V., & Lokeshwari, D. M. (2015). Pyrans: Heterocycles of chemical and biological interest. *Journal of Chemical and Pharmaceutical Research, 7*(11), 693–700.

Ma, C., Hong, F., & Yang, S. (2022). Amyloidosis in Alzheimer's disease: Pathogeny, etiology, and related therapeutic directions. *Molecules, 27*(4), Article 1210. https://doi.org/10.3390/molecules27041210

Mahdavi, S. M., Habibi, A., Dolati, H., Shahcheragh, S. M., Sardari, S., & Azerang, P. (2018). Synthesis and antimicrobial evaluation of 4H-pyrans and schiff bases fused 4H-pyran derivatives as inhibitors of Mycobacterium bovis (BCG). *Iranian Journal of Pharmaceutical Research: IJPR, 17*(4), 1229.

Omar, S. H., Scott, C. J., Hamlin, A. S., & Obied, H. K. (2017). The protective role of plant biophenols in mechanisms of Alzheimer's disease. *The Journal of Nutritional Biochemistry, 47*, 1–20. https://doi.org/10.1016/j.jnutbio.2017.02.016

Ow, S.-Y., & Dunstan, D. E. (2014). A brief overview of amyloids and Alzheimer's disease. *Protein Science, 23*(10), 1315–1331. https://doi.org/10.1002/pro.2524

Perluigi, M., Di Domenico, F., & Butterfield, D. A. (2024). Oxidative damage in neurodegeneration: Roles in the pathogenesis and progression of Alzheimer disease. *Physiological Reviews, 104*(1), 103–197. https://doi.org/10.1016/j.redox.2023.103057

Pourshojaei, Y., Abiri, A., Eskandari, R., Dourandish, F., Eskandari, K., & Asadipour, A. (2019). Synthesis, biological evaluation, and computational studies of novel fused six-membered O-containing heterocycles as potential acetylcholinesterase inhibitors. *Computational Biology and Chemistry, 80*, 249–258. https://doi.org/10.1016/j.ejmech.2019.04.005

Rajmohan, R., & Reddy, P. H. (2017). Amyloid-beta and phosphorylated tau accumulations cause abnormalities at synapses of Alzheimer's disease neurons. *Journal of Alzheimer's Disease, 57*(4), 975–999. https://doi.org/10.3233/JAD-160612

Sharma, S., Brahmachari, G., Banerjee, B., Kant, R., & Gupta, V. K. (2015). X-ray studies of methyl 6-amino-5-cyano-2-methyl-4-(3-nitrophenyl)-4H-pyran-3-carboxylate. *European Chemical Bulletin, 4*(5), 230–233. https://doi.org/10.1134/S1063774515050236

Sojoudi, M., & Mokhtary, M. (2018). Efficient one-pot synthesis of 6-amino-4-aryl-5-cyano-2-methyl-4H-

pyran-3-carboxylates catalyzed by nano MgO in water. *Quarterly Journal of Iranian Chemical Communication, 6*(2), 125–133. https://doi.org/10.22034/IJC.2018.55797.1306

Winblad, B., Amouyel, P., Andrieu, S., Ballard, C., Brayne, C., Brodaty, H., *et al.* (2016). Defeating Alzheimer's disease and other dementias: A priority for European science and society. *The Lancet Neurology, 15*(5), 455–532. https://doi.org/10.1016/S1474-4422(16)30055-9

How to cite this paper:

Nasiri, S, Arasteh, A. & Mokhtary, M. (2026). 6-Amino-4H-pyran derivatives as potential anti-microbial and amyloid aggregation inhibitory agents. *Microbiology, Metabolites and Biotechnology, 9*(1), x-xx.
DOI: 22104/mmb.2026.8200.1202